Nonlinear Impact-Echo Test for Quantitative Evaluation of ASR Damage in Concrete

Clayton Malone[1] · Hongbin Sun[2] · Jinying Zhu[1]

Abstract

Nonlinear acoustic methods demonstrate high sensitivity for concrete damage evaluation. Among these methods, nonlinear resonance acoustic methods have been widely used in laboratory tests on small scale test samples. In this study, a nonlinear impact-echo (IE) method for concrete damage evaluation was introduced, in which the IE frequency shift was measured at different impact force levels. The nonlinear IE test and the nonlinear impact resonance acoustic spectroscopy (NIRAS) test share similarities in the experimental setup and analysis method. However, the nonlinear IE test excites a local thickness resonance mode of a member instead of the global resonance vibration. Therefore, the analyzed mode is unaffected by member boundary conditions and is applicable to large concrete structural members. To identify the fundamental IE frequencies, multiple impacts were applied along the members. Once the fundamental IE frequencies were determined, the effectiveness of the nonlinear IE method was evaluated by testing seven concrete beam specimens with varying levels of alkali-silica reaction (ASR) damage. The nonlinear IE test demonstrates high sensitivity to concrete damage and allows for quantitative assessment of the damage state of concrete without a baseline measurement.

Keywords Nonlinear · Acoustics · Impact-echo · Alkali-silica reaction · Concrete

1 Introduction

Nonlinear acoustic techniques have gained attention in the nondestructive testing (NDT) field because they are more sensitive to microcracking damage than linear acoustic methods. In materials with complex microstructures, such as concrete, microcracks smaller than the aggregates might not cause a significant change of linear acoustic parameters (wave velocity, resonance frequencies), but they will induce high acoustic nonlinearity. Nonlinear acoustic responses may include material softening with strain [1], higher harmon-

✉ Jinying Zhu
  jyzhu@unl.edu

  Clayton Malone
  cmalone@huskers.unl.edu

  Hongbin Sun
  sunh1@ornl.gov

[1] Department of Civil and Environmental Engineering, University of Nebraska Lincoln, 1110 S 67TH ST, Omaha, NE 68118, USA

[2] Oak Ridge National Laboratory, P.O. Box 2008, Oak Ridge, TN 37831, USA

ics [2], or side band frequencies [3]. Softening is shown as a decrease of the Young's modulus with increasing strain, which can be measured by monitoring the change in resonance frequency [1] or wave velocity [4] under different strain levels.

The nonlinear resonance acoustic spectroscopy (NRAS) method [1] is a common nonlinear acoustic laboratory test. During NRAS testing, the resonance frequency shift Δf is measured when a sample is excited by frequency sweeps around the resonance frequency at different strain levels. Chen et al. [5] proposed generating the resonance flexural mode of a sample through a hammer impact and measuring the resonance frequency shift under different impact amplitudes. This method is called "Nonlinear Impact Resonance Acoustic Spectroscopy" (NIRAS), which can be regarded as a nonlinear adaptation of the resonant frequency test in accordance with ASTM C215 [6]. The NIRAS method is simple in test setup and analysis. In both NRAS and NIRAS methods, the strain levels are very low, so an accelerometer is typically used to measure the resonant response (acceleration). A relative nonlinear parameter is typically measured as the slope of the relationship between relative frequency shift and impact amplitude or acceleration response amplitude [5,

7]. Dynamic acoustoelastic testing (DAET) measures ultrasonic wave velocity changes due to dynamic modulation by a low frequency (LF) acoustic wave [8–10]. Nonlinear parameters are extracted from the correlation curves between the relative velocity change of ultrasonic pulses and the instantaneous LF amplitude (or strain). The DAET method provides more details about hysteresis, transient elastic softening, and slow relaxation than the vibration based methods.

Although these nonlinear ultrasonic testing methods show different degrees of success in laboratory tests, there are several major limitations that hinder application of these methods in practice. First, these tests are only applicable to small samples. The NRAS test needs to excite the free vibration of the tested sample, and DAET uses a shake table or large piezoelectric disk to vibrate the sample to generate internal strain changes. These methods are difficult to apply to large concrete structures. Second, because global free vibration modes are excited, the resonance frequency and nonlinear response not only depend on material properties and specimen dimensions, but also depend on boundary and support conditions. These tests cannot simply be extended to concrete structural members because of various types of end supports in real structures. Some recent studies have applied nonlinear ultrasonic tests to large-scale concrete specimens and structures with promising results [11, 12], but these methods either need high power input sources or the results for damage evaluation are qualitative.

A common NDT method used to evaluate plate structures is the impact-echo (IE) test [13]. Application of the IE test has also been extended to other structures, such as columns and beams [14, 15]. The IE test is convenient, as it only requires access to one side of the member being tested. In the case of a plate, the measured IE frequency is only dependent on the thickness. For beams and columns, the measured IE frequency depends on the aspect ratio of the cross-section. These factors allow the IE test to be readily applied to large scale concrete members. The IE test can be used to assess concrete damage development, where a drop in frequency or wave velocity is monitored over time. However, solely monitoring these parameters is inadequate for quantitative characterization of concrete damage. In order to employ linear parameters like frequency or wave velocity for quantitative characterization, it is necessary to have a reference baseline measurement. However, baseline measurements on field specimens are often not readily available, which limits the ability of using the IE test for damage assessment.

This paper introduces a nonlinear IE method for concrete damage evaluation. The nonlinear IE test uses impacts of increasing force to generate the fundamental IE mode of concrete members, resembling the NIRAS test, which measures the resonance frequency of small test samples. As multiple impacts of increasing force are applied, the

shift in the fundamental IE frequency is measured. Specimen damage is monitored by tracking a relative nonlinear parameter that is found by taking the slope of the linear-fit correlation between the relative IE frequency shift and acceleration response amplitude. A control concrete specimen and specimens with different levels of alkali-silica reaction (ASR) damage were studied using the nonlinear IE method to evaluate the method's effectiveness for concrete damage assessment.

2 Theoretical Background of Resonance Modes in Bars

2.1 Linear Impact-Echo Theory

In a plate, the IE test measures a local resonance mode with a frequency related to the thickness h and the P wave velocity V_P of a member as $f = \beta_{IE} V_P / 2h$. Gibson and Popovics [16] proved that the local resonance mode is a non-propagating Lamb wave S_1 mode at the zero-group-velocity (S_1ZGV), and the parameter β_{IE} (known as the shape factor) only depends on Poisson's ratio. Higher order ZGV modes may also be detectable in a plate, such as the A_2ZGV mode, but the S_1ZGV mode dominates in most cases. Prada et al. [17] presented an extensive study on the existence of ZGV modes and their frequencies for different Poisson's ratios.

The IE test has also been applied to beams and columns [14, 15]. Similar to plates, these modes also correspond to ZGV modes or cutoff frequency modes (zero wavenumber) [18]. The ZGV frequencies can be obtained from dispersion curves by solving the dispersion equation for cylindrical structures. Dispersion curves for a bar with a non-cylindrical cross-section should be solved using a semi-analytical finite element method [19]. Unlike in plates, there are many ZGV and cut-off frequencies in a rod within a narrow frequency range. Therefore, a hammer impact on a beam or column often excites multiple modes. The fundamental mode is typically analyzed. For beams and columns, the IE frequencies can still be expressed in the form of $f = \beta_{IE} V_P / 2D$ [15], where D represents the thickness of the specimen in the direction being tested, and β_{IE} is dependent on the cross-section geometry (circle, square, or rectangle) and Poisson's ratio of the specimen. Lin and Sansalone found that square cross-sectioned concrete members have a β_{IE} value of around 0.87 [14] for the fundamental IE mode, which increases slightly with a smaller Poisson's ratio.

2.2 Nonlinear Acoustic Theory

Concrete is a material that exhibits nonlinear behavior. The arrangement and interaction of the various components of the concrete microstructure (cement paste, aggregates, pores,

and cracks) in the mesoscopic range (10^{-6} to 10^{-9} m) are responsible for its nonlinearity. When cracks and microcracks are present, concrete experiences a significant increase in nonlinearity. The presence of nonlinearity in concrete can be observed in the hysteresis found in its stress–strain relationship and in the discrete memory effect [20]. The strain and strain rate-dependent modulus of concrete can be described by the following nonlinear hysteresis model [21]:

$$E(\varepsilon, \dot{\varepsilon}) = E_0 \left\{ 1 - \beta\varepsilon - \delta\varepsilon^2 - \alpha \left[\Delta\varepsilon + \varepsilon\,\text{sign}(\dot{\varepsilon}) \right] \right\}, \quad (1)$$

where E_0 is the linear modulus, $\Delta\varepsilon$ is the local strain amplitude over the previous period, $\dot{\varepsilon}$ is the strain rate, β is the quadratic nonlinear parameter, δ is the cubic nonlinear parameter, and α is the hysteresis parameter. The function $\text{sign}(\dot{\varepsilon})$ takes the value of 1 if $\dot{\varepsilon} > 0$ and -1 if $\dot{\varepsilon} < 0$. Note that the quadratic nonlinear parameter β is unrelated to the IE shape factor β_{IE}.

Nonlinear acoustic techniques are more sensitive to microdamage than linear acoustic methods. Equation 1 describes the principle underlying many nonlinear acoustic methods, where the elastic modulus decreases (softening) with increasing strain. Nonlinear acoustic methods typically induce larger strain levels (10^{-6} to 10^{-5}) in materials compared to their linear counterparts (10^{-7}) [22]. The nonlinearity is found in changes to acoustic properties (i.e., frequency or velocity) under varying strain levels [22]. This is exemplified in the NRAS method, where the relative resonance frequency shift is correlated with the change in strain ($\Delta\varepsilon$) as [1]:

$$\frac{f_0 - f}{f_0} = \alpha_\varepsilon \Delta\varepsilon, \quad (2)$$

where f_0 is the linear resonant frequency measured at a low strain level and f is the frequency at a higher strain level. It should be noted that the relative nonlinear parameter α_ε is proportional to the absolute nonlinear parameter α that is found in Eq. 1 [1]. Measuring the strain (ε) can be challenging, so it is common in lab experiments to measure other output parameters when determining the nonlinear parameter. In nonlinear ultrasonic tests, typically the specimen response is measured with an accelerometer [23] or the particle velocity is measured with a laser vibrometer [24]. In nonlinear impact tests, the impact force from an instrumented hammer [5] or the amplitude of the acceleration response signals collected with an accelerometer [7] are typically used. In this study, a relative nonlinear parameter (α_a) was measured from the relationship between the normalized frequency shift $\left(\frac{f_0 - f}{f_0} \right)$ and the amplitude of the acceleration (m/s^2) signals from the hammer impacts. For simplicity, the parameter α referred to thereafter in this paper is the relative nonlinear parameter α_a, that has the units of s^2/m.

Plane Strain – Mode 1
Frequency = 6319 Hz

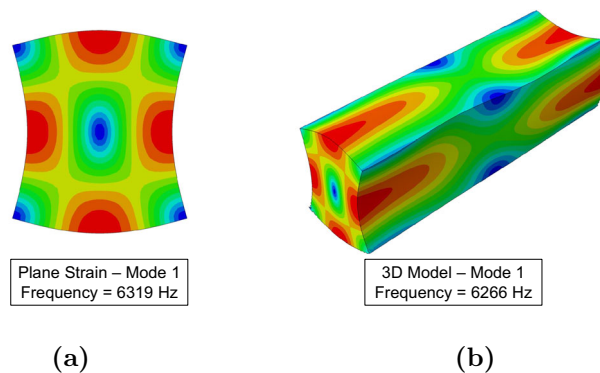3D Model – Mode 1
Frequency = 6266 Hz

(a)   (b)

Fig. 1 Numerical simulations showing the fundamental IE mode of **a** the 2D (plane strain) model ($f = 6319$ Hz) and **b** the 3D model ($f = 6266$ Hz)

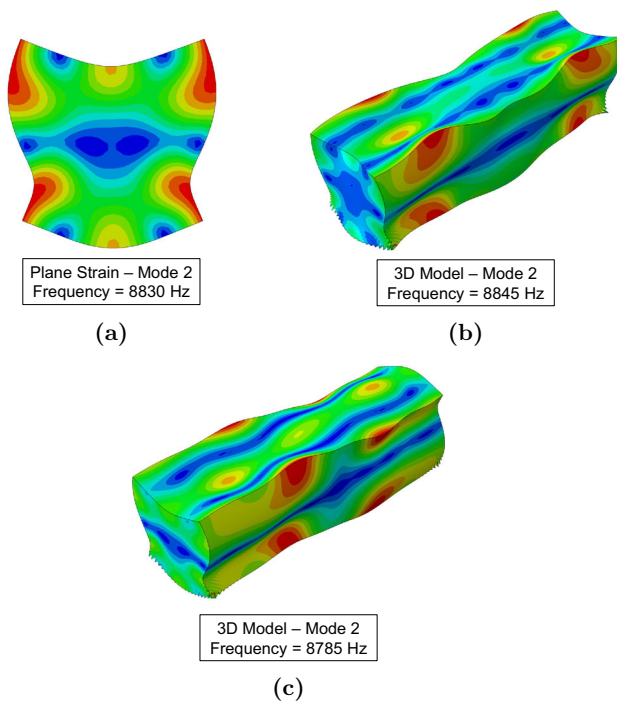## 2.3 Nonlinear Impact-Echo

Unlike global vibration modes, the local resonance modes measured in the IE test are not affected by boundary conditions. Therefore, the IE test is applicable to large size concrete plates, beams, and columns. By extending the nonlinear resonance theory in Eq. 2 and the NIRAS test method to the IE test, a nonlinear acoustic test can be performed on large concrete specimens. When multiple impacts are applied to the specimen, the IE frequency will decrease as the impact amplitude increases. It is possible to perform a substitution in Eq. 1, replacing the strain with dynamic response parameters such as velocity or acceleration, since the maximum strain and the maximum velocity/acceleration are linearly related [23].

3 Finite Element Simulations

Finite element simulations were conducted using Abaqus® to confirm the fundamental IE modes tested in this study. Modal analyses were performed on 2D (0.30 m × 0.30 m) and 3D concrete models (0.30 m × 0.30 m × 1.10 m) with a mesh size of 8 mm. The material properties used in the simulation were as follows: density $\rho = 2410$ kg/m^3, Young's modulus $E = 40{,}000$ MPa, and Poisson's ratio $\nu = 0.15$. These parameters give a P-wave velocity (V_p) of approximately 4200 m/s, which agrees with the experimental values measured on the concrete specimens in this study.

Figure 1 shows the fundamental IE modes using the 2D (plane strain) and 3D models, which give the IE frequencies of 6319 Hz and 6266 Hz, respectively. The frequency of the 2D model represents the cutoff frequency (zero wavenumber), while the frequency from the 3D model represents a local ZGV mode. The β_{IE} parameter is calculated as 0.89 for the given material properties.

Plane Strain – Mode 2
Frequency = 8830 Hz

(a)

3D Model – Mode 2
Frequency = 8845 Hz

(b)

3D Model – Mode 2
Frequency = 8785 Hz

(c)

Fig. 2 Numerical simulations showing the second IE mode of **a** the 2D (plane strain) model ($f = 8830$ Hz), **b** the 3D model ($f = 8845$ Hz), and **c** an IE mode involving a 180° rotation at one end of the beam ($f = 8785$ Hz)

Figure 2a and b show the second IE mode of the 2D (plane strain) and 3D models, with frequencies of 8830 Hz and 8845 Hz, respectively. The frequency ratio between the second and fundamental IE modes observed in the 3D models is $f_2 = 1.41 f_1$, aligning with the findings reported by Lin and Sansalone [14]. Furthermore, these frequencies agree with the measured frequencies of the concrete specimens in this study. More details will be discussed in Sect. 5.1. The numerical simulation shows another resonance mode near the second IE mode, as seen in Fig. 2c. This mode is also found in the experiments in this study, when the impact distance moved farther away from the receiver. The modes in Figs. 1b and Fig. 2b are symmetric in the longitudinal direction, while the mode in Fig. 2c involves a 180° rotation at one end of the beam.

4 Concrete Specimens and NDT Experimental Setup

4.1 Concrete Specimens

In this project, seven specimens of various mix designs, lengths, and damage levels were tested to evaluate the effectiveness of the nonlinear IE test in quantitatively characterizing concrete damage. All specimens have a cross-section
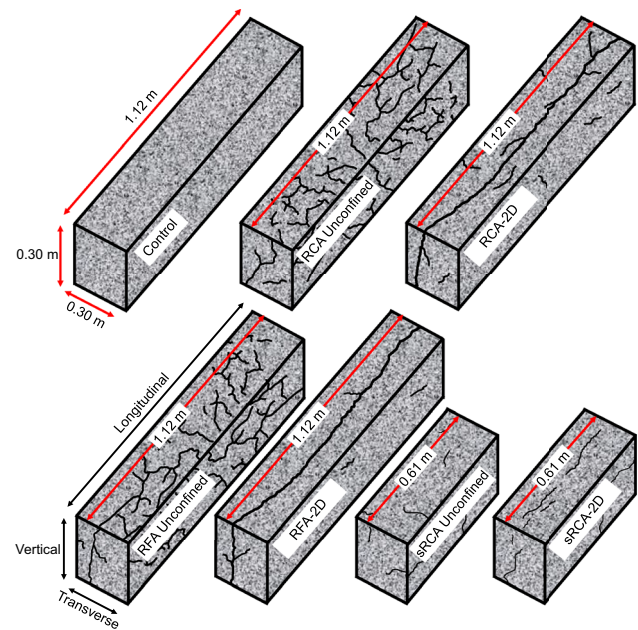
Fig. 3 Specimen design of Control, RCA Unconfined, RCA-2D, RFA Unconfined, RFA-2D, sRCA Unconfined, and sRCA-2D specimens

of 0.30 m × 0.30 m. In all confined specimens ("2D" specimens), #6 (diameter: 19 mm) headed reinforcement steel bars were used to constrain the expansion in the longitudinal and vertical directions. The specimen design along with the Cartesian axes for what is referred to as the longitudinal, transverse, and vertical directions throughout this study are shown in Fig. 3.

Three different concrete mix designs (see Table 1) were utilized: (1) a control mix using innocuous local coarse and fine aggregates, (2) a reactive mix using a reactive coarse aggregate (RCA) and an innocuous local fine aggregate, and (3) a reactive mix using a reactive fine aggregate (RFA) and an innocuous local coarse aggregate. NaOH was added to the reactive mixes, boosting the alkali content to 1.50% Na_2O_{eq} by mass of cement. One unconfined control specimen was tested, and each unconfined ASR damaged specimen has a 2D confined counterpart. Two of the seven specimens tested had a shorter length of 0.61 m, while the rest were 1.12 m. The two shorter specimens (sRCA and sRCA-2D) were cast with reactive coarse aggregate. Details of all seven specimens are summarized in Table 2. These specimens were cast and tested by Malone and others during his thesis work. Information regarding the specimens and test results in addition to what is presented in this paper can be found in Malone's thesis [25].

All specimens were moist cured for at least 28 days after casting. Then the specimens were moved to an environmental chamber for high temperature (38 °C) and high humidity (95% RH) conditioning. The specimens were placed on carts to ensure all surfaces were exposed to moisture. An image

Table 1 Concrete mix design (SSD) and strength

Component	Control (kg/m^3)	RCA (kg/m^3)	RFA (kg/m^3)
Cement	350	350	350
Water	175	175	175
Coarse aggregate	1127	1039	1095
Fine aggregate	709	839	743
Water reducer	2.3 mL/kg	2.3 mL/kg	2.3 mL/kg
50/50 NaOH	0	9.31	9.31
w/c	0.50	0.50	0.50
28-day strength	37.2 MPa	32.7 MPa	32.8 MPa

Table 2 Concrete specimen information

Specimen	Dimension (m)	Mix design	Conditioning start date
Control	0.30 × 0.30 ×1.12	Control	11/27/2018
RCA Unc., RCA-2D	0.30 × 0.30 × 1.12	RCA	11/27/2018
RFA Unc., RFA-2D	0.30 × 0.30 × 1.12	RFA	04/04/2019
sRCA Unc., sRCA-2D	0.30 × 0.30 × 0.61	RCA	08/20/2019

of the seven test specimens in the environmental chamber is shown in Fig. 4. Demountable mechanical strain gauges (DEMEC) were used to measure specimen expansions in the vertical, transverse, and longitudinal directions. Stainless steel DEMEC targets were epoxied on all surfaces (except for the bottom) of each specimen and in two directions on each surface. Every 2 weeks, the chamber was shut down overnight and then maintained at 23 °C and 50% RH for 24 h. Expansion measurements and IE testing were performed during the shutdown period when the internal temperature of the concrete specimens reached a stable temperature of 23 °C. Expansion measurements were conducted using 150 mm and 500 mm DEMEC strain gauges (Mayes Instruments Limited, UK). Three expansion measurements were taken in each direction on the specimens and were averaged. After all measurements were completed, the chamber was restarted, and the temperature and humidity resumed conditioning at 38 °C and 95% RH.

The measured expansion of each test specimen throughout the conditioning period is shown in Fig. 5. For the unconfined specimens, the expansion in the vertical and transverse directions are averaged, whereas the 2D reinforced specimen's vertical and transverse directional expansions are displayed separately as the confinement caused different damage in each direction. IE testing began on the same date for all specimens, but because the specimens were cast at different times, the conditioning ages of specimens were different. The beginning of the IE testing period is indicated in Fig. 5. Therefore, when the IE test began, the ASR specimens were in early, intermediate, and late stages of damage. By monitoring these specimens for more than 200 days, data was captured to evaluate the entire progression of ASR development.

4.2 Impact-Echo Mode Determination

During IE testing, a typical hammer (200 g) was used to impact the concrete specimens. The responses from the hammer impacts were recorded using an accelerometer (PCB 352C65) that was powered by a signal conditioner (Brüel & Kjær 1704). The sensitivity of the accelerometer was 10.2 mV/(m/s^2). The impact response signals were digitized by an oscilloscope (PicoScope 4262) with a sampling frequency of 100 kHz. A LabVIEW program was designed to control the data acquisition process. The program displays and saves the raw impact response time-domain signals and amplitude spectra. In the nonlinear IE test, the user can monitor the spectra to ensure increasing amplitude during successive impacts. The saved signals were then imported in MATLAB for linear or nonlinear analysis. When performing Fourier transform (FFT), the time domain signals were zero-padded to improve the frequency resolution.

When an impact is applied to a beam member, it can excite multiple IE modes and global vibration modes. Confidently determining which mode, or peak, in the frequency spectrum corresponds to the fundamental IE mode can be challenging in such cases. Global vibration modes are affected by the impact location, support conditions, and beam length. The IE mode is independent of support conditions and can consistently be observed at each impact location. Consequently, a reliable approach for identifying the IE mode involves performing multiple impacts along the specimen and analyzing the resulting signals collectively. This proposed multi-impact technique enables conclusive determination of the fundamental IE frequency. The experimental setup for IE mode determination is shown in Fig. 6a. To minimize any boundary effects, the accelerometer was positioned at a distance

Fig. 4 Top surface of **a** Control, **b** RCA Unconfined, **c** RCA-2D, **d** RFA Unconfined, **e** RFA-2D, **f** sRCA Unconfined, and **g** sRCA-2D specimens. Images were taken at the end of the monitoring program

Control
(a)

RCA Unconfined
(b)

RCA-2D
(c)

RFA Unconfined
(d)

RFA-2D
(e)

sRCA Unconfined
(f)

sRCA-2D
(g)
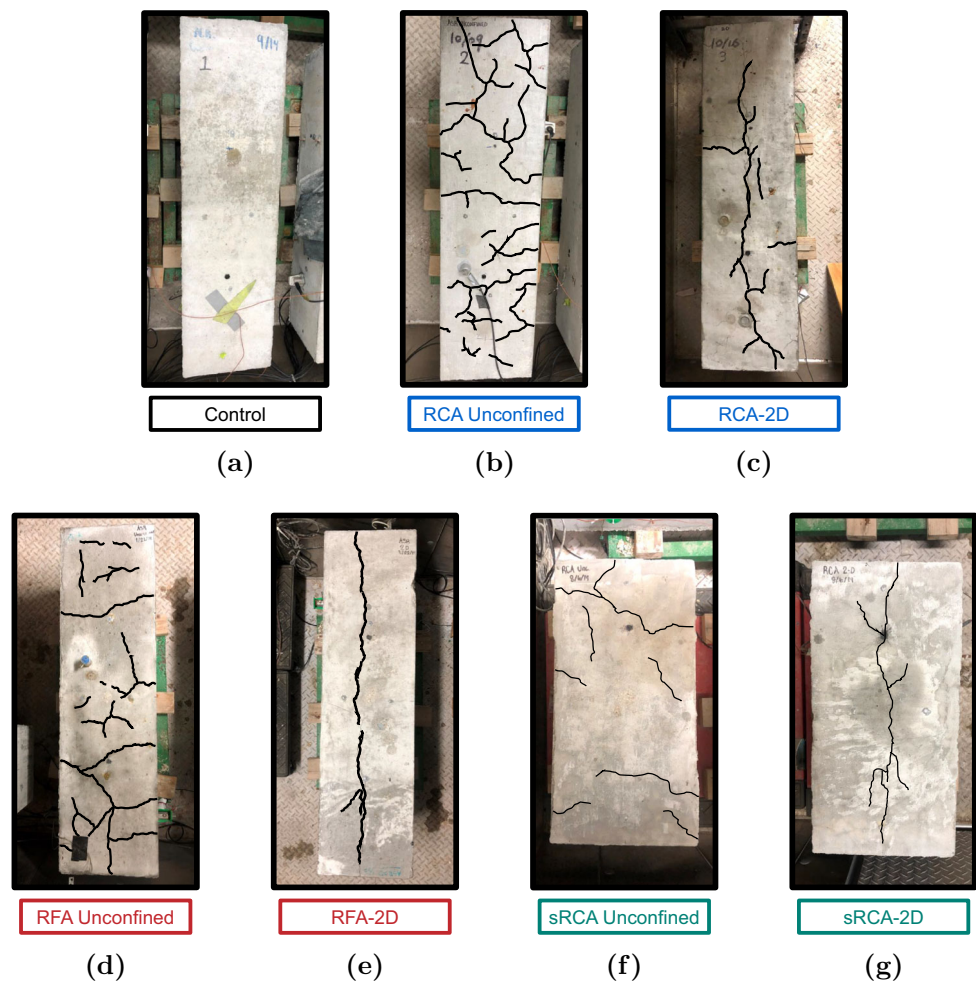
of 35 cm from the end of the 1.12 m specimen. Similarly, for the 0.61 m specimen, the accelerometer was placed 15 cm from the end. Impacts were applied to the specimen at 5 cm intervals. Tests were performed in two directions, vertical and transverse, on each specimen. The vertical direction refers to impacts performed perpendicular to the top surface of the specimens. Likewise, the transverse direction refers to impacts performed perpendicular to the side surfaces of the specimens.

4.3 Nonlinear Impact-Echo Test Setup

After the IE frequency was determined, the nonlinear IE test was conducted in the vertical and transverse directions on each specimen. The experimental setup for the nonlinear IE test is shown in Fig. 6b. The accelerometer was fixed at the center position on the side of the beam being tested and was not moved throughout the test. Multiple impacts were conducted at a distance of approximately 5 cm from the accelerometer with increasing impact amplitudes. The test procedure is similar to the NIRAS method. As the impact amplitude increases, the IE frequency decreases. The non-

linearity of the specimen is determined as the slope of the linear-fit line relating the acceleration response amplitude and IE frequency shift.

For the 2D confined specimens, the nonlinear IE test was conducted on the top surface by impacting in the vertical direction and side surface by impacting in the transverse direction. Due to the confinement in the vertical and longitudinal directions, the ASR damage in each direction was distinct. For the unconfined specimens, it was found that the two directions showed similar nonlinear IE results because the ASR damage was uniform. Therefore, for the unconfined specimens, the nonlinear IE results in the vertical and transverse directions were averaged and taken as representative of the overall damage state of the specimen.

Figure 7a illustrates the procedure of stacking multiple frequency domain signals obtained from three different specimen types (Control, sRCA Unconfined, and RCA Unconfined). As specimen damage increased, a larger shift in IE frequency was observed with increasing impact amplitude. To determine the nonlinear parameter (α), the relationship between the resonance frequency shift ($f_0 - f)/f_0$ and the acceleration response amplitude was plotted. The slope of
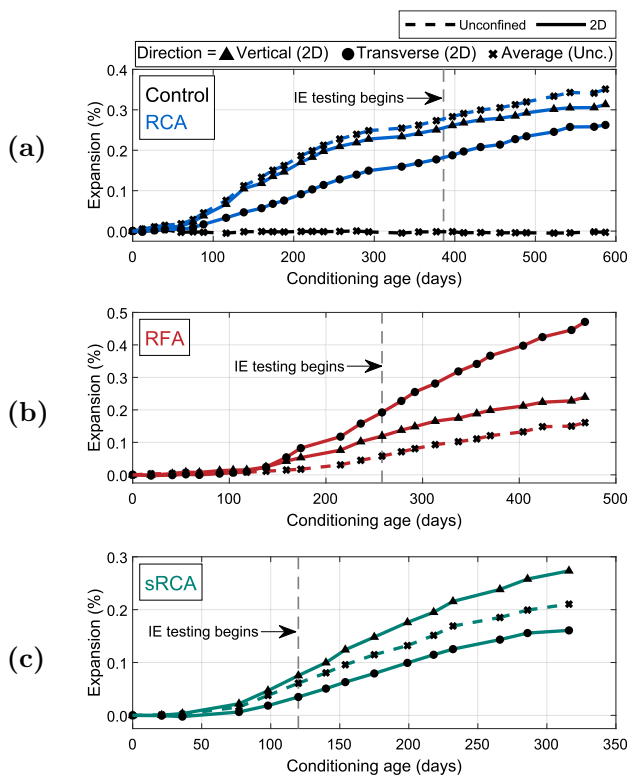
Fig. 5 Expansion measurement results during specimen conditioning for **a** Control, RCA Unconfined, RCA-2D, **b** RFA Unconfined, RFA-2D, and **c** sRCA Unconfined, and sRCA-2D specimens in vertical and transverse directions for 2D confined specimens and the average of vertical and transverse directions for unconfined specimens
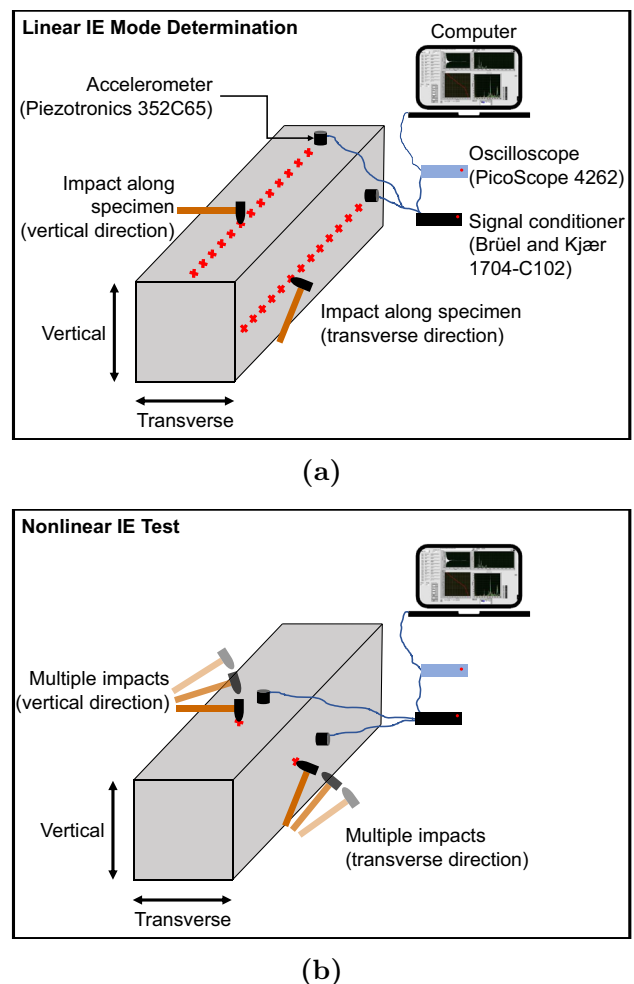
this relationship was calculated to obtain the value of α. This process is illustrated in Fig. 7b.

Fig. 6 Experimental setup for **a** linear impact-echo mode determination and **b** nonlinear impact-echo testing

5 Results and Discussion

5.1 Impact-Echo Mode Determination

Figure 8a shows a typical frequency spectrum generated from an impact applied to the Control specimen in the vertical direction, along with a 2D frequency spectrum color image created by stacking frequency-domain signals obtained from several impacts performed along the length of the beam. Results from tests performed in the vertical direction on the sRCA unconfined and RFA-2D specimens are also displayed in Fig. 8b and c, respectively. The frequency spectrum of the specific impact displayed for each specimen is marked with a dashed line in the corresponding 2D frequency spectrum image.
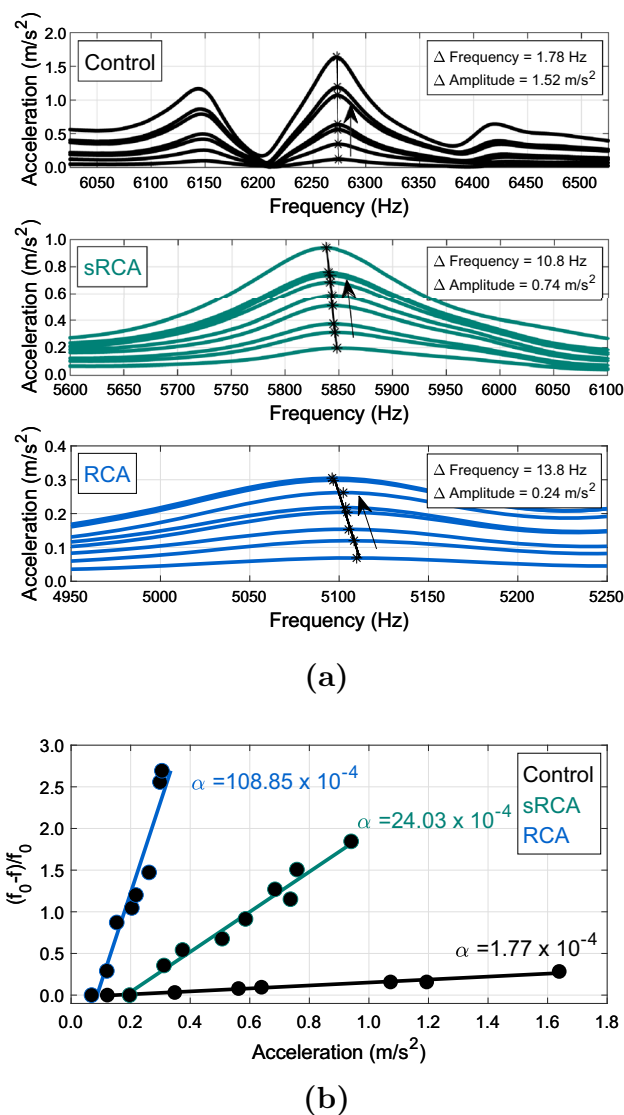
In Fig. 8a, the first vertical strip, which varied from 6221 to 6269 Hz, represents the fundamental IE mode of the Control specimen. The second vertical strip represents the second IE mode (found at a frequency of approximately $f_2 = 8850$ Hz). Similar to the results of the numerical analysis (see Sect. 3), the frequency ratio between the second and fundamental IE modes observed in the specimens is $f_2 = 1.41 f_1$, aligning with the findings reported by Lin and Sansalone [14]. The numerical simulation predicts another mode that is very similar to the second IE mode but at a slightly lower frequency. This is observed as the second strip shifts to the left from 8848 to 8776 Hz when the impact was applied at a large distance (> 75 cm). The third strip does not correspond to any mode in the numerical simulation. Therefore, it may be a global vibration mode for the specific beam length and support conditions.

Figure 8b shows a typical frequency spectrum generated from an impact applied to the sRCA Unconfined specimen in the vertical direction. The first vertical strip in the 2D image, which varied from 6071 to 6104 Hz, represents the fundamental IE mode. The second vertical strip represents the second IE mode (found at a frequency of approximately $f_2 = 8815$ Hz). Figure 8(c) shows a typical frequency spec-

(a)

(b)

Fig. 7 Impact-echo signals and analysis including **a** frequency spectra and **b** multi-impact nonlinear analysis for the following specimens in the respective testing directions: Control vertical direction (vertical expansion of −0.007%), sRCA Unconfined transverse direction (transverse expansion of 0.057%), and RCA Unconfined transverse direction (transverse expansion of 0.209%) from tests performed on 01/08/2020

trum generated from an impact on the RFA-2D specimen in the vertical direction. The first vertical strip in the 2D image, which varied from 5500 to 5586 Hz, represents the fundamental IE mode. The second vertical strip represents the second IE mode (found at a frequency of approximately $f_2 = 7810$ Hz).

The fundamental IE mode of the RFA-2D specimen (average frequency of $f_1 = 5555$ Hz) was found to be approximately 11% less than that of the Control specimen (average frequency of $f_1 = 6255$ Hz) at the time of the tests performed in Fig. 8. It can also be seen that B-scan images of the two ASR damaged specimens, sRCA Unconfined and RFA-2D,

are less clear than the B-scan of the Control specimen indicating increased damping. However, since the specimen IE frequency is dependent on its dimensions and material properties (velocity, density, modulus, Poisson's ratio), it is not possible to draw a conclusion about the damage state of the specimens from these features. Nevertheless, as displayed in Fig. 8, by performing impacts along the beams and generating the B-scan image, the fundamental IE mode can be clearly seen.

The specimens in this study have a square cross-section, so the fundamental IE mode is easy to identify using the presented method. For more complex cases, time–frequency analysis and the multichannel analysis of surface waves (MASW) method [26] can be used to build the dispersion curves to identify the cutoff and ZGV frequencies.

5.2 Linear Impact-Echo Results

The fundamental IE mode frequency was used in both linear and nonlinear analyses. In the nonlinear IE test, a series of impacts with progressively increasing amplitudes were applied. The peak IE frequency observed from the impact with the lowest amplitude was considered to be the linear IE frequency for each specimen.

Figure 9 presents the progression of the linear IE frequency of all specimens with the conditioning age over the monitoring period. The average linear Control IE measurement ($f = 6255$ Hz) was taken as a representative baseline for all seven specimens, because the IE frequency of the Control specimen was stable throughout the entire monitoring period. The normalized linear IE frequency was calculated by expressing the linear IE frequency of each specimen as a percentage relative to the average Control linear IE frequency.

Although the specimens were cast at different dates and have different confinement conditions, the data shows a clear decreasing trend with conditioning age. Because the IE monitoring started after 100 days of conditioning on the sRCA specimens, the initial frequency drop date was not captured, which may indicate the initiation of ASR expansion. By extrapolating the data to the earlier date, it is found that the frequency drop started around 80 days of conditioning. The IE frequency decreased fast in the first 400 to 500 days, and then generally became saturated as it approached 80%, although specimen expansion was still progressing (as seen in Fig. 5). The influence of cracking on the elastic modulus of the specimens reached a maximum, and further development of damage no longer had a noticeable impact on the linear IE frequency. This result is consistent with previous findings for resonance frequency testing on ASR damaged concrete prisms by Malone et al. [27], Rivard and Saint-Pierre [28], and Giannini et al. [29]. A study monitoring the relative ultrasonic velocity change in the same group of specimens by Sun
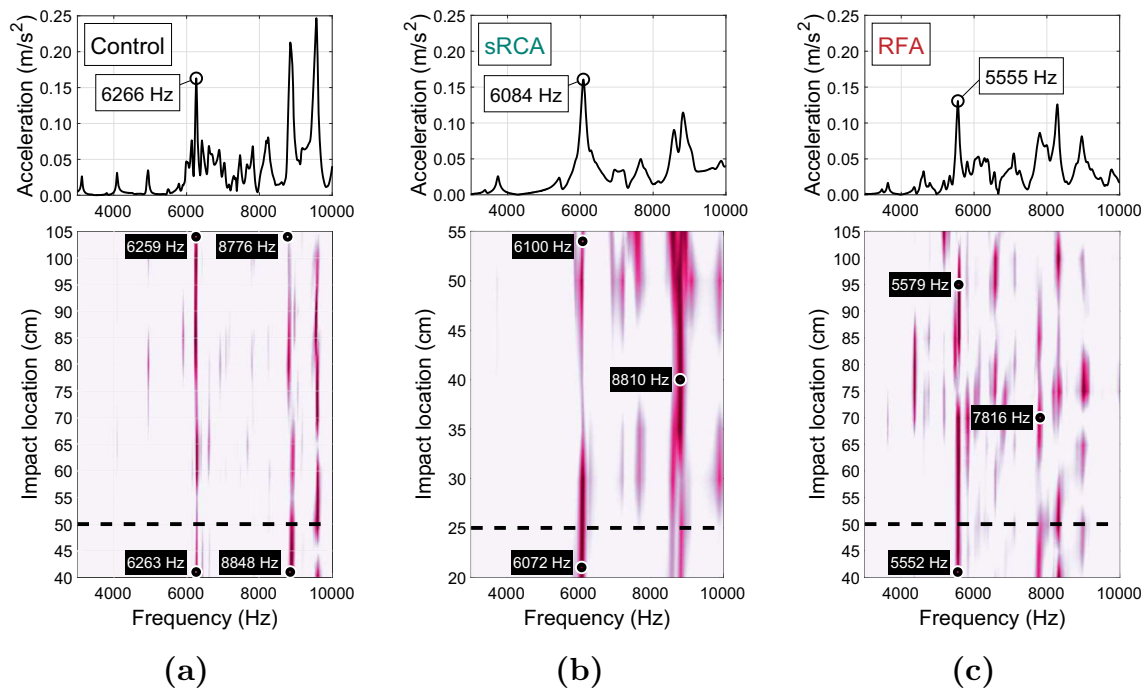
Fig. 8 Frequency spectrum from a single impact (top row) and multi impact analysis B-scan image (bottom row) for **a** the Control specimen (vertical expansion of −0.008%) (average fundamental IE mode f_1 = 6255 Hz), **b** sRCA Unconfined specimen (vertical expansion of 0.021%) (average fundamental IE mode f_1 = 6084 Hz), and **c** RFA-2D specimen (vertical expansion of 0.068%) (average fundamental IE mode f_1 = 5555 Hz). The frequency spectrum of the specific impact displayed in the top row is marked with a dashed line in the 2D frequency spectrum image shown in the bottom row. All results presented were performed in vertical direction
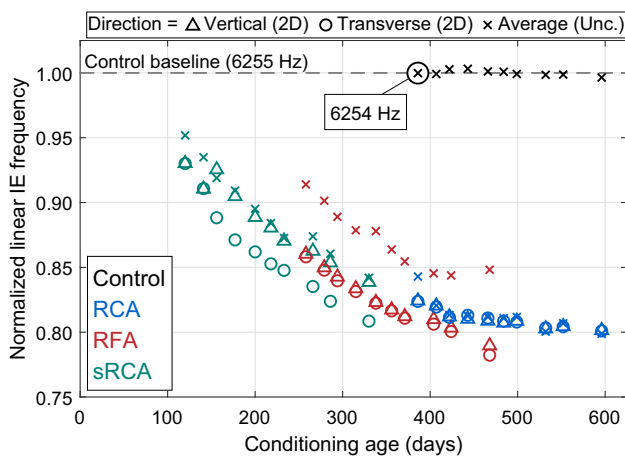
Fig. 9 Normalized linear IE frequency for all specimens. Frequencies in vertical and transverse directions are plotted for 2D confined specimens, and the average frequency in vertical and transverse directions are plotted for unconfined specimens

et al. [30] also indicated saturation at a velocity drop of 20%. In this study, however, the final measurement on the RFA-2D specimen dropped below 80%. This may be in part due to the large longitudinal crack that opened in the specimen near the end of the test period (see Fig. 4), resulting in the RFA-2D

transverse direction having the largest expansion among all specimens in this study (see Fig. 5).

The IE frequency of a specimen is dependent on its dimensions and material properties (velocity, density, modulus, Poisson's ratio). Slight variations in specimen dimensions or materials will affect the IE frequency. The IE frequency progression of the six ASR specimens follow the same general trend, except the trend of the RFA Unconfined data is shifted higher than the rest of the test specimens. Ideally, a baseline IE frequency measurement is available for each specimen. The baseline frequency data is not available in this study, so the IE frequency of the Control specimen was used for normalization. If the RFA Unconfined specimen had a higher initial frequency, normalization by the Control specimen's frequency would shift the data higher. Therefore, drawing a conclusion about the health of the specimen by directly comparing IE frequencies is not feasible. To be able to interpret the damage state of the specimen, a baseline measurement is needed.

5.3 Nonlinear Impact-Echo Results

The nonlinear IE test was performed during the conditioning period to monitor specimen damage development. Microcracking present from ASR increased the material non-
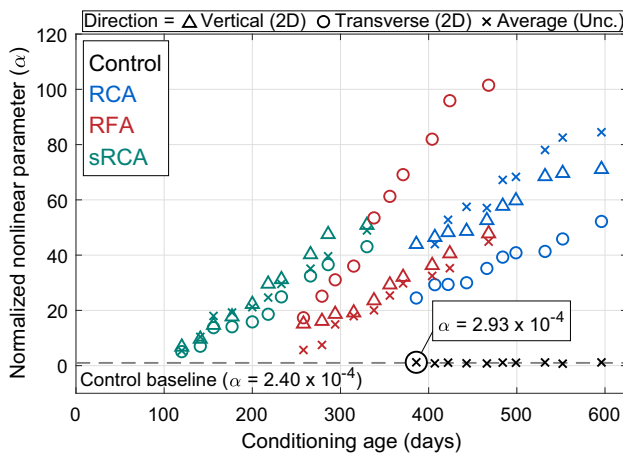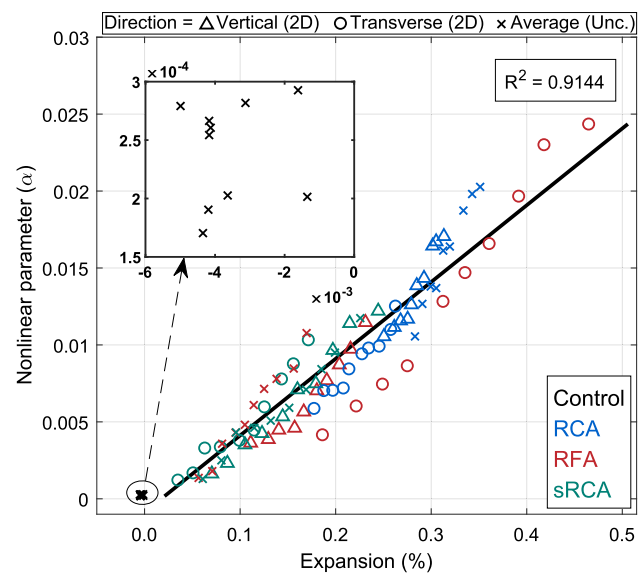
Fig. 10 Normalized nonlinear IE measurement results for all specimens in vertical and transverse directions for 2D confined specimens and the average of vertical and transverse directions for unconfined specimens

Fig. 11 Relationship between nonlinear parameter (α) and specimen expansion for the Control, RCA Unconfined, RCA-2D, RFA Unconfined, RFA-2D, sRCA Unconfined, and sRCA-2D specimens in vertical and transverse directions for 2D confined specimens and the average of vertical and transverse directions for unconfined specimens

linearity, due to clapping and friction at the crack interfaces under external excitement. Figure 10 plots the progression of the normalized nonlinear parameter (α) with conditioning age for the Control, RCA Unconfined, RCA-2D, RFA Unconfined, RFA-2D, sRCA Unconfined, and sRCA-2D specimens. Results were normalized to the average nonlinear parameter value of the Control specimen ($\alpha = 2.40 \times 10^{-4}$). For the reactive specimens, as the conditioning time increased, both the damage and the nonlinear parameter determined by nonlinear IE testing experienced a corresponding increase.

At the end of monitoring, the nonlinear parameter in all reactive specimens increased 50 to 100 times compared to the Control specimen. The Control specimen did not show any damage, and the nonlinear parameter had negligible change and remained around a value of $\alpha = 2 \times 10^{-4}$ during the testing period. The results indicate that the nonlinear IE test is sensitive to detecting damage in concrete specimens, even at late ages. The measured nonlinear parameter increased throughout the whole duration of the test and did not become saturated past a certain damage level, unlike the linear IE results.

The six ASR damaged specimens followed the same general rate of nonlinear parameter increase during the testing period, except for the transverse direction of the RFA-2D specimen. The parameter in the transverse direction of the RFA-2D specimen increased at a significantly faster rate than in other specimens. Looking at Fig. 5, the transverse direction expansion of the RFA-2D specimen was the largest among the ASR damaged specimens. This expansion can be practically seen in Fig. 4, where a large crack in the longitudinal direction is shown on the top surface of the RFA-2D specimen as a result of substantial transverse expansion. The increased damage in this direction resulted in a higher measurement of nonlinear parameter throughout the testing period.

5.4 Quantitative Correlation of Nonlinear Results and ASR Expansion

Figure 11 presents the relationship between the nonlinear parameter of all specimens and their respective directional expansions over the course of the testing period. The results across all specimens form a nearly linear relationship, regardless of their mix design, length, or reactive aggregate type. The strong linear correlation indicates that the specimen's expansion and nonlinear behavior may both be governed by the same parameter related to the ASR damage during the monitoring period, crack density. A comparable finding was also observed on a study on small concrete prisms using the NIRAS test [27], in which the prisms had similar mix designs as the large specimens in this study. Comparing the relationship between specimen nonlinearity and expansion with the previous study on small prisms, this study shows more variance. This can likely be explained by increased material variation across the specimens, as the different beam specimens in this study were cast in separate batches. The expansion measurements may also contribute to the variation. For prisms, unlike the specimens in this study, the expansion can be measured across the full length of the specimen and is likely more uniform, as there is no presence of rebar. Finally, the frequency spectra during IE testing are complicated and include several modes. When other modes are close to the fundamental IE mode, error may be introduced when selecting the peak frequency and its amplitude. This error is

minimized when performing the NIRAS test on small prisms, as the flexural mode clearly dominates.

The repeatability of this test is presented in the consistency of the measurements on the Control specimen over the entire testing period. A total of ten nonlinear IE tests were performed on each specimen over the testing period. As there was no damage development in the Control specimen, it was assumed that the nonlinearity of the specimen would remain relatively unchanged. Over the course of the testing period, the values of nonlinear parameter on the six ASR damaged specimens ranged from $\alpha = 12.2 \times 10^{-4}$ to 244×10^{-4}. However, the values of nonlinear parameter on the Control specimen only ranged from $\alpha = 1.70 \times 10^{-4}$ to 2.93×10^{-4}, with a mean value $(\bar{X}) = 2.40 \times 10^{-4}$ and standard deviation $(\sigma) = 0.42 \times 10^{-4}$. The low variance in the measurements on the Control specimen (displayed in Fig. 11), taken over more than 200 days, instills confidence in the consistency and repeatability of the nonlinear IE test.

The relationship observed in the ASR specimens suggests the potential for utilizing the nonlinear IE method to quantitatively assess ASR damage by correlating the nonlinear parameter to specimen expansion. Unlike an expansion measurement or the linear IE test, which require a baseline value, the nonlinear parameter from the nonlinear IE test can be determined without having a reference measurement available. The measured nonlinear parameter displays a high sensitivity to specimen cracking while remaining unaffected by other properties such as specimen length or aggregate type and is therefore suitable for quantitative evaluation of ASR damage.

6 Conclusions

This paper presents the nonlinear IE test for concrete ASR damage evaluation. The proposed nonlinear IE method combines the practical benefits of the IE test with the heightened sensitivity of nonlinear acoustic analysis. In doing so, it provides a practical solution for evaluating large concrete specimens. The effectiveness of the nonlinear IE method was validated on concrete beam specimens of varying lengths, with different degrees of ASR damage. Major findings from the study are presented below:

(1) The nonlinear IE test method is convenient and simple to apply, and the acquired results are independent of the support condition and length of the specimen being tested. For those reasons, this method is suitable for evaluating damage in large specimens.

(2) Many vibration modes are excited in beam or column members by an impact. Therefore, it is sometimes challenging to identify the fundamental IE mode. In this study, multiple impacts were applied along the speci-

mens and the frequency spectra were stacked to identify the IE modes.

(3) Monitoring the fundamental linear IE frequency over the testing period allowed for evaluation of ASR damage in the concrete specimens. However, a baseline measurement is needed. In addition, across most specimens in the study, the IE frequency drop became saturated at approximately 20% and stopped decreasing, although the ASR damage was still progressing. Therefore, linear analysis of IE test signals is useful only when a baseline measurement is available and when concrete damage is in early or medium stages.

(4) The nonlinear IE method is highly sensitive to ASR damage and was used to evaluate the damage state of six different ASR damaged specimens in this study. The largest nonlinear parameter occurred in the RFA-2D specimen in the transverse direction, with a final value of $\alpha = 244 \times 10^{-4}$ (at a transverse expansion of 0.465%). This value is approximately 100 times greater than the average value observed in the Control specimen. The nonlinear parameter continued to increase proportionally to damage development and did not become saturated, while the linear frequency reached a maximum decrease and became inadequate for monitoring any further progression of damage. This phenomenon has been observed in other linear resonance tests and ultrasonic wave velocity monitoring of ASR specimens.

(5) The test results display a nearly linear relationship between the nonlinear IE parameter and ASR expansion that could be utilized to assess the level of damage in a specimen without the need for a baseline measurement. The relationship indicates the results obtained from the nonlinear IE test are related to the presence of cracking and are not influenced by specimen length or aggregate type. While the tests in this study were performed on square cross-sectioned beam members, the authors believe its application can be extended to plates and other structural members that have similar thickness resonance modes. Therefore, the proposed nonlinear IE test has potential to be applied in the evaluation of concrete structures.

Author Contributions JZ and CM conceptualized the methodology. CM collected data and performed analysis. All authors wrote, edited, and reviewed the manuscript.

Data Availability The data that support the findings of this study are available from the corresponding author J.Z. upon reasonable request.

Declarations

Conflict of interest The corresponding author Jinying Zhu is an Associate Editor of Journal of Nondestructive Evaluation.

Consent for Publication The publisher has the author's permission to publish this paper and the research findings within it. Results in this paper are based on the work in the first author's Master Thesis [25].

Code Availability The code is available upon reasonable request.

References

1. Van Den Abeele, K.E.A., Carmeliet, J., Ten Cate, J.A., Johnson, P.A.: Nonlinear elastic wave spectroscopy (NEWS) techniques to discern material damage, Part II: single-mode nonlinear resonance acoustic spectroscopy. J. Res. Nondestruct. Eval. **12**(1), 31–42 (2000)
2. Breazeale, M., Thompson, D.: Finite-amplitude ultrasonic waves in aluminum. Appl. Phys. Lett. **3**(5), 77–78 (1963)
3. Eiras, J., Kundu, T., Bonilla, M., Payá, J.: Nondestructive monitoring of ageing of alkali resistant glass fiber reinforced cement (GRC). J. Nondestruct. Eval. **32**, 300–314 (2013)
4. Zhang, Y., Tournat, V., Abraham, O., Durand, O., Letourneur, S., Le Duff, A., et al.: Nonlinear mixing of ultrasonic coda waves with lower frequency-swept pump waves for a global detection of defects in multiple scattering media. J. Appl. Phys. **113**(6), 064905 (2013)
5. Chen, J., Jayapalan, A.R., Kim, J.Y., Kurtis, K.E., Jacobs, L.J.: Rapid evaluation of alkali-silica reactivity of aggregates using a nonlinear resonance spectroscopy technique. Cem. Concr. Res. **40**(6), 914–923 (2010)
6. ASTM: ASTM Standard C215 Standard Test Method for Fundamental Transverse, Longitudinal, and Torsional Resonant Frequencies of Concrete Specimens. ASTM, West Conshohocken (2019)
7. Leśnicki, K.J., Kim, J.Y., Kurtis, K.E., Jacobs, L.J.: Characterization of ASR damage in concrete using nonlinear impact resonance acoustic spectroscopy technique. NDT E Int. **44**(8), 721–727 (2011)
8. Renaud, G., Callé, S., Defontaine, M.: Remote dynamic acoustoelastic testing: elastic and dissipative acoustic nonlinearities measured under hydrostatic tension and compression. Appl. Phys. Lett. **94**(1), 011905 (2009)
9. Renaud, G., Talmant, M., Callé, S., Defontaine, M., Laugier, P.: Nonlinear elastodynamics in micro-inhomogeneous solids observed by head-wave based dynamic acoustoelastic testing. J. Acoust. Soc. Am. **130**(6), 3583–3589 (2011)
10. Shokouhi, P., Rivière, J., Lake, C.R., Le Bas, P.Y., Ulrich, T.: Dynamic acousto-elastic testing of concrete with a coda-wave probe: comparison with standard linear and nonlinear ultrasonic techniques. Ultrasonics **81**, 59–65 (2017)
11. Zhang, Y., Larose, E., Moreau, L., d'Ozouville, G.: Three-dimensional in situ imaging of cracks in concrete using diffuse ultrasound. Struct. Health Monit. **17**(2), 279–284 (2018). https://doi.org/10.1177/1475921717690938
12. Basu, S., Thirumalaiselvi, A., Sasmal, S., Kundu, T.: Nonlinear ultrasonics-based technique for monitoring damage progression in reinforced concrete structures. Ultrasonics **115**, 106472 (2021). https://doi.org/10.1016/j.ultras.2021.106472
13. ASTM: ASTM Standard C1383. Standard Test Method for Measuring the P-Wave Speed and the Thickness of Concrete Plates Using the Impact-Echo Method. ASTM, West Conshohocken (2015)
14. Lin, Y., Sansalone, M.: Transient response of thick circular and square bars subjected to transverse elastic impact. J. Acoust. Soc. Am. **91**(2), 885–893 (1992)
15. Sansalone, M.J., Streett, W.B.: Impact-Echo: Nondestructive Evaluation of Concrete and Masonry. Bullbrier Press, Ithaca (1997)
16. Gibson, A., Popovics, J.S.: Lamb wave basis for impact-echo method analysis. J. Eng. Mech. **131**(4), 438–443 (2005)
17. Prada, C., Clorennec, D., Royer, D.: Local vibration of an elastic plate and zero-group velocity Lamb modes. J. Acoust. Soc. Am. **124**(1), 203–212 (2008). https://doi.org/10.1121/1.2918543
18. Laurent, J., Royer, D., Hussain, T., Ahmad, F., Prada, C.: Laser induced zero-group velocity resonances in transversely isotropic cylinder. J. Acoust. Soc. Am. **137**(6), 3325–3334 (2015). https://doi.org/10.1121/1.4921608
19. Hayashi, T., Song, W.J., Rose, J.L.: Guided wave dispersion curves for a bar with an arbitrary cross-section, a rod and rail example. Ultrasonics **41**(3), 175–183 (2003). https://doi.org/10.1016/S0041-624X(03)00097-0
20. Guyer, R.A., McCall, K.R., Boitnott, G.N.: Hysteresis, discrete memory, and nonlinear wave propagation in rock: a new paradigm. Phys. Rev. Lett. **74**(17), 3491–3494 (1995)
21. Van Den Abeele, K.E.A., Johnson, P.A., Sutin, A.: Nonlinear elastic wave spectroscopy (NEWS) techniques to discern material damage, Part I: nonlinear wave modulation spectroscopy (NWMS). J. Res. Nondestruct. Eval. **12**(1), 17–30 (2000)
22. Jin, J., Moreno, M.G., Riviere, J., Shokouhi, P.: Impact-based nonlinear acoustic testing for characterizing distributed damage in concrete. J. Nondestruct. Eval. **36**(3), 51 (2017)
23. Johnson, P.A., Zinszner, B., Rasolofosaon, P.N.: Resonance and elastic nonlinear phenomena in rock. J. Geophys. Res. Solid Earth **101**(B5), 11553–11564 (1996)
24. Payan, C., Ulrich, T.J., Le Bas, P.Y., Saleh, T., Guimaraes, M.: Quantitative linear and nonlinear resonance inspection techniques and analysis for material characterization: application to concrete thermal damage. J. Acoust. Soc. Am. **136**(2), 537–546 (2014)
25. Malone, C.: Quantitative Assessment of Alkali-Silica Reaction in Small and Large-Scale Concrete Specimens Utilizing Nonlinear Acoustic Techniques. University of Nebraska-Lincoln, Lincoln (2020)
26. Bjurström, H., Ryden, N.: Detecting the thickness mode frequency in a concrete plate using backward wave propagation. J. Acoust. Soc. Am. **139**(2), 649–657 (2016). https://doi.org/10.1121/1.4941250
27. Malone, C., Zhu, J., Hu, J., Snyder, A., Giannini, E.: Evaluation of alkali-silica reaction damage in concrete using linear and nonlinear resonance techniques. Constr. Build. Mater. **303**, 124538 (2021)
28. Rivard, P., Saint-Pierre, F.: Assessing alkali-silica reaction damage to concrete with non-destructive methods: from the lab to the field. Constr. Build. Mater. **23**(2), 902–909 (2009)
29. Giannini, E.R., Folliard, K.J., Zhu, J., Bayrak, O., Kreitman, K., Webb, Z., et al.: Non-destructive Evaluation of In-service Concrete Structures Affected by Alkali-Silica Reaction (ASR) or Delayed Ettringite Formation (DEF)—Final Report, Part I. FHWA/TX-13/0-6491-1 (2013). http://library.ctr.utexas.edu/ctr-publications/0-6491-1.pdf
30. Sun, H., Tang, Y., Malone, C., Zhu, J.: Long-term ultrasonic monitoring of concrete affected by alkali-silica reaction. Struct. Health Monit. (2023). https://doi.org/10.1177/14759217231169000